

Figure 1. Polarized IR spectra of stretched fibers ( $M_w = 5\,000\,00$ ): broken line,  $\perp$ ; solid line,  $\parallel$ .

$$f = \frac{R - 1}{R_0 - 1} \frac{R_0 + 2}{R + 2}$$

where  $R$  and  $R_0$  are the observed and ideal dichroic ratios, respectively. From the dichroic ratios observed in stretched samples for suitable vibrations of the PEO chains which we may assume to be either parallel or perpendicular to the stretched axis, the  $f$  parameter was found to be 0.81. This value was very close to the one obtained in the case of stretched intercalates previously studied.<sup>8</sup> We note here that this simplified model cannot be used to account for the dispersion in orientation of crystals in a peripheral part of a spherulite. Pleochroism measurements on doubly oriented specimens were carried out by recording FTIR spectra at various incidence angles with nonpolarized light.

**Attributions of IR Bands of pnp.** The attributions of IR absorption bands were based on different studies relative to substituted aromatic molecules. From the studies of Randle and Whiffen,<sup>9</sup> Stephenson et al.,<sup>10</sup> Green et al.,<sup>11</sup> and Pinchas et al.<sup>12</sup> on nitrobenzene derivatives, the attributions of the  $\text{NO}_2$  vibrations were made (see Table 1). We can note here that the dichroism observed in uniaxially oriented samples may provide insight into the IR modes of vibration. For instance, rocking and asymmetric stretching vibrations of  $\text{NO}_2$  have their transition moment parallel to each other. Therefore these two vibrations must have the same dichroism. We can see in the IR spectra of the stretched complex (Figure 1) that the 531- and 1512- $\text{cm}^{-1}$  bands have the same dichroism behavior. These observations lead to the conclusion that the 531- $\text{cm}^{-1}$  band corresponds to the rocking  $\text{NO}_2$  vibration. The pnp molecules belong to the  $C_{2v}$  symmetry group. A trirectangular  $X$ ,  $Y$ , and  $Z$  system is attached to the pnp molecule. The  $Z$  axis was taken as the 1-4 axis, the  $Y$  axis is in the plane of the benzene ring normal to the 1-4 axis, and finally the  $X$  axis corresponds to the out-of-plane vibrations of the benzene ring. The vibrations polarized along  $Z$ ,  $Y$ , and  $X$  belong to the  $a_1$ ,  $b_1$ , and  $b_2$  irreducible representations, respec-

Table 1. Attributions of the  $\text{NO}_2$  and Aromatic Ring Vibrations for the pnp Molecules

Attributions and Wavenumbers (cm <sup>-1</sup> ) of NO <sub>2</sub> Vibrations				
Randle and Whiffen <sup>9</sup>	Stephenson et al. <sup>10</sup>	Green et al. <sup>11</sup>	Pinchas et al. <sup>12</sup>	
	wag 442	rock 420	rock 417	
	rock 533	wag 532	wag 532	
$\nu(\text{CN})$ 854	sciss 853	$\nu(\text{CN})$ 852	sciss 850	
$\nu_s$ 1353	$\nu_s$ 1351	$\nu_s$ 1351	$\nu_s$ 1349	
$\nu_{as}$ 1534	$\nu_{as}$ 1527	$\nu_{as}$ 1527	$\nu_{as}$ 1531	
Symmetries, Attributions, and Wavenumbers (cm <sup>-1</sup> ) of Aromatic Vibrations				
Garrigou- Lagrange et al. <sup>13</sup>	Stephenson et al. <sup>10</sup>	Green et al. <sup>11</sup>	Evans <sup>15</sup>	Green et al. <sup>14</sup>
	a <sub>1</sub> -6a-397	a <sub>1</sub> -1-397		a <sub>1</sub> -379
	b <sub>2</sub> -17b-508	b <sub>2</sub> -16b-420	b <sub>2</sub> -508	b <sub>2</sub> -16b-507
	a <sub>1</sub> -1-680	a <sub>1</sub> -6a-677		
b <sub>2</sub> -4-680	b <sub>2</sub> -4-703	b <sub>2</sub> -4-704	b <sub>2</sub> -690	b <sub>2</sub> -4-699
	b <sub>2</sub> -11-795		b <sub>2</sub> -753	
			a <sub>1</sub> -812	
b <sub>2</sub> -17b-850		a <sub>1</sub> -6a-852		b <sub>2</sub> -11-817
				b <sub>2</sub> -5-922
a <sub>1</sub> -9a-1170	a <sub>1</sub> -9a-1176	a <sub>1</sub> -9a-1174		a <sub>1</sub> -9a-1170
b <sub>1</sub> -19b-1450		b <sub>1</sub> -19b-1412	b <sub>1</sub> -1474	b <sub>1</sub> -1428
a <sub>1</sub> -19a-1490	a <sub>1</sub> -19a-1482	a <sub>1</sub> -19a-1475	a <sub>1</sub> -1500	a <sub>1</sub> -19a-1515
b <sub>1</sub> -8b-1570	b <sub>1</sub> -8b-1590	b <sub>1</sub> -8b-1585	b <sub>1</sub> -1597	b <sub>1</sub> -1598
a <sub>1</sub> -8a-1590	b <sub>1</sub> -(12+6b)- 1608	a <sub>1</sub> -8a-1603	a <sub>1</sub> -1604	a <sub>1</sub> -8a-1615

tively. Our attributions were based on the study of Garrigou-Lagrange et al.<sup>13</sup> on 34 disubstituted aromatic molecules, on the work of Stephenson, et al.<sup>10</sup> and Green et al.<sup>11</sup> on nitrobenzene, and finally on the work of Green et al.<sup>14</sup> and Evans<sup>15</sup> on substituted phenols. The attributions are summarized in Table 1. As we will show later, these attributions are consistent with the dichroism observed in our various samples.

**Normal Mode Analyses.** To confirm which vibrations are characteristic of the polymer in the spectra of the PEO-pnp complex, we have observed the isotopic shifts when deuterated polymer, instead of hydrogenated PEO, is used as the host component. The calculations of the normal modes of the PEO chains in the various possible conformations were made by using Wilson's GF matrix method.<sup>16</sup> The G matrix was calculated according to Schimanouchi's scheme.<sup>17</sup> The force constants used by Tadokoro<sup>18</sup> for the study of the vibrations of PEO in the 7/2 helical conformation were adopted without considering the hydrogen bonding between host and guest molecules on any intermolecular interactions.

## Results and Discussion

**Orientation of the pnp Molecules.** We first discuss the modifications in the IR spectra of the pnp molecules induced by the complexation. In the case of intercalates made of PEO and  $p$ -dihalogenobenzenes, some IR absorption bands of the aromatic molecules were found to be shifted in the IR spectra.<sup>8</sup> For the pnp, we do not observe any shift of the IR bands except for the vibrations characteristic of hydrogen bonds. For instance, the OH stretching vibration appears at 3320  $\text{cm}^{-1}$  for the pure pnp and at 3271  $\text{cm}^{-1}$  for the complex. This observed red shift clearly shows that the interactions are stronger between PEO and pnp than between pnp molecules.<sup>19</sup> The orientation of the pnp molecules in the unit cell will be found by the measurement of dichroic ratios in stretched fibers and in spherulitic samples. First, X-ray diffraction studies previously reported<sup>3</sup> have shown that the stretched fibers have the  $c$  crystallographic parameter along the fiber axis and that the crystal growth front in the spherulites used corresponds to the (100) crystallographic plane.

**Stretched Samples.** Figure 1 shows the polarized IR spectra of a stretched sample of complex. The observed

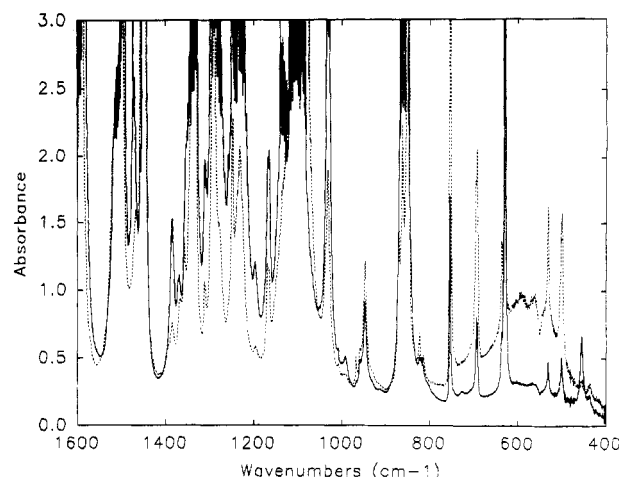
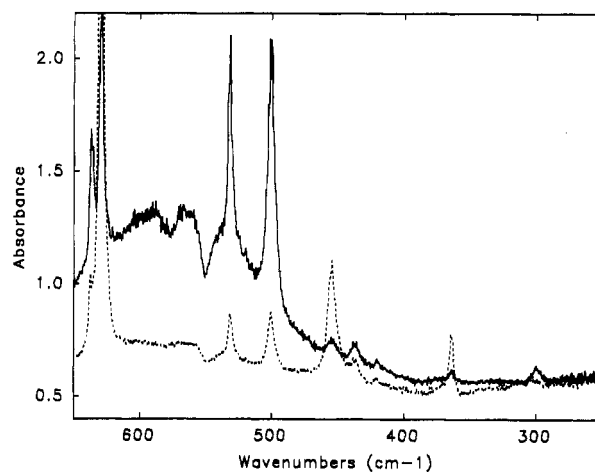
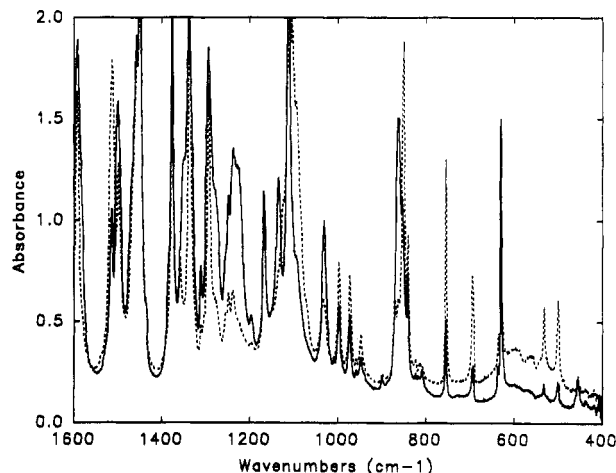
**Table 2. Attributions, Dichroic Ratios, and  $\alpha$  Angles Observed for pnp IR Bands for Stretched Fibers of PEO ( $M_w = 500000$ )-pnp Complex**

mode	wavenumber (cm <sup>-1</sup> )	dichroic ratio	$\alpha_{\text{corr}}^a$ (deg)
<b>a<sub>1</sub></b>			
20a	364	0.11	88
6a	630	0.13	88
9a	1166	0.33	72
19a	1500	0.21	78
8a	1612	0.13	88
<b>b<sub>1</sub></b>			
16b	501	11.3	10
10b	635	14.0	1
4	694	12.7	7
11	755	9.1	15
17b	851		
5	959		
<b>b<sub>2</sub></b>			
19b	1448	0.21	78
8b	1589	⊥	
20b	3084		
$\nu(\text{OH})$	3271	0.07	90
wag	437	5.3	25
rock	531	6.0	23
sciss	863	0.06	90
$\nu_{\text{as}}$	1512	2.8	37

<sup>a</sup>  $\alpha$  corrected for sample dispersion.

dichroic ratios for the pnp molecules are given in Table 2. The  $f$  parameter determined from PEO IR bands is equal to 0.81. With this value, the  $\alpha$  angles between the transition moment of vibrations and the fiber axis, the  $c$  crystallographic parameter, can be calculated. From Table 2, we can see that the b<sub>2</sub> vibrations, which have their transition moment normal to the benzene ring, are all polarized parallel to the fiber axis and the a<sub>1</sub> and b<sub>1</sub> vibrations, which have their transition moment in the plane of the benzene ring, are all polarized perpendicular to the fiber axis. The average values obtained for the angles  $\alpha_x$ ,  $\alpha_y$ , and  $\alpha_z$  are equal to 8, 78, and 83°, respectively. We may conclude that the benzene ring is very nearly perpendicular to the  $c$  crystallographic parameter. The dichroism of the IR bands characteristic of the nitro group gives us confidence in these observations. In fact, the out-of-plane NO<sub>2</sub> wagging is polarized parallel to the fiber axis, and the in-plane NO<sub>2</sub> scissoring and OH stretching are polarized perpendicular to the fiber axis. On the other hand, the observed dichroism for the NO<sub>2</sub> rocking and asymmetric stretching shows that the plane of the NO<sub>2</sub> group is not parallel to the benzene ring. The observed dichroic ratios give an angle of 40° between the two planes. Similar results were obtained for pure pnp in the  $\beta$  modification crystalline form.<sup>20</sup>

**Spherulitic Fibers.** Complete determination of the orientation of the pnp molecules requires the study of a sample with a fiber axis different from the  $c$  axis of a stretched fiber. A PEO-pnp spherulite is a complex aggregate of lamellae in which a well-defined crystallographic axis is oriented along the radial direction. The X-ray diffraction pattern of a peripheral part of a spherulite (Figure 7) shows that the fiber axis (growth direction) corresponds to the  $a^*$  reciprocal parameter. This means that the (100) planes are perpendicular to the radius of the spherulite and that the crystals are randomly oriented around this direction. We may therefore consider that a peripheral part of a spherulite is approximately uniaxially oriented like a fiber with the  $a^*$  reciprocal parameter along the fiber axis. Figures 2 and 3 show the polarized IR spectra obtained for a spherulite of PEO( $M_w = 200000$ )-pnp and for a spherulite PEO( $M_w = 6000$ )-pnp, respectively. The samples made from low molecular

**Figure 2.** Polarized IR spectra of a peripheral part of a (100) spherulite ( $M_w = 200\,000$ ): broken line,  $\perp$ ; solid line,  $\parallel$ .**Figure 3.** Polarized IR spectra of a peripheral part of a (100) spherulite ( $M_w = 6000$ ) between PP foils: broken line,  $\perp$ ; solid line,  $\parallel$ .

weight PEO required a mechanical support; we chose to use thin polypropylene (PP) foils for this purpose. From the observed dichroic ratios given in Table 3, we can consider that the a<sub>1</sub> vibrations, which have their transition moment along the Z direction (1-4 axis of the pnp molecule), are polarized parallel to the radius of the spherulite ( $a^*$ ), with dichroic ratios within the range 2.2-5.7. On the other hand, the b<sub>1</sub> and b<sub>2</sub> vibrations, which have their transition moments along the X and Y axes, are polarized perpendicular to the radius of the spherulite, with dichroic ratios within the range 0.36-0.27. This implies that the 1-4 axis of the pnp molecules is very likely parallel to the  $a^*$  reciprocal parameter. The observed

**Table 3. Attributions, Dichroic Ratios, and  $\alpha$  Angles Observed for pnp IR Bands for Peripheral Part of a Spherulite of PEO ( $M_w = 20000$ )-pnp and PEO ( $M_w = 6000$ )-pnp Complexes**

mode	wavenumber (cm <sup>-1</sup> )	PEO( $M_w=6000$ )-pnp		PEO( $M_w=20000$ )-pnp	
		dichroic ratio	$\alpha$ (deg)	dichroic ratio	$\alpha$ (deg)
a <sub>1</sub>					
20a	364	5.7	31	2.0	45
6a	630	2.85	40		
9a	1166				
19a	1500	2.2	44		
8a	1612	2.1	44		
b <sub>2</sub>					
16b	501	0.36	67	0.27	70
10b	635	0.33	68	⊥	
4	694	0.27	70	0.37	67
11	755	0.33	68	⊥	
17b	851	⊥			
5	959			0.25	71
b <sub>1</sub>					
8b	1589	1.2	52		
20b	3084	0.31	69	0.29	69
$\nu(\text{OH})$	3271	6.21	30		
wag	437	0.66	60		
rock	531	0.22	72	0.23	71
sciss	863	17.5	19		
$\nu_{\text{as}}$	1512	0.31	69		

dichroic ratios depart significantly from the expected values for a perfect fiber. This is because the dispersion in the orientation of the crystals with respect to the spherulite radius may be noticeable, and, moreover, due to the extent of the incident IR beam, we do not observe a single spherulitic fiber. Thus we cannot account for the dispersion of orientation with the simplified model of Fraser. The dichroic behavior of the NO<sub>2</sub> IR bands gives us confidence in our conclusions. The NO<sub>2</sub> scissoring, which has its transition moment along the 1-4 axis, is polarized parallel to the radius of the spherulite, and the NO<sub>2</sub> rocking, asymmetric stretching, and wagging, which have their transition moments normal to the 1-4 axis, are all polarized perpendicular to the radius ( $\alpha^*$ ). Thus the study of the dichroism of the IR bands of pnp in the spherulites shows that the 1-4 axis of the molecules is preferentially aligned with the  $\alpha^*$  reciprocal parameter. Additional arguments are obtained from X-ray evidence. First, despite the fact that the unit cell is triclinic, the  $\alpha$  and  $\beta$  angles do not depart significantly from 90°; the (004) reflection appears to be much more intense than any other (00*l*) reflections in the X-ray diffraction pattern of the stretched specimen. Second, the length of the *c* parameter (1.557 nm), which is related to the height of a stack of 4 pnp molecules,<sup>3</sup> is in accordance with the thickness of a benzene ring (more or less 0.38 nm). We have then completely determined the orientation of the pnp molecules in the unit cell. The benzene rings are very likely normal to the *c* crystallographic parameter, and the 1-4 axis of the pnp molecules is roughly parallel to the  $\alpha^*$  reciprocal parameter. The pnp orientation is given in Figure 9. To complete the description of the crystalline structure of the PEO-pnp complex, the conformation adopted by the PEO molecules must now be determined.

**Conformation of the PEO Chains.** In the FTIR spectra of a molecular complex such as the PEO-pnp system, we observe both the IR vibrations of the pnp molecules, analyzed here above, and those of the PEO chains. To distinguish without any doubt what IR bands are characteristic of the PEO chains, we used the isotopic shifts observed when complex specimens are prepared with the deuterated instead of the hydrogenated polymer. The

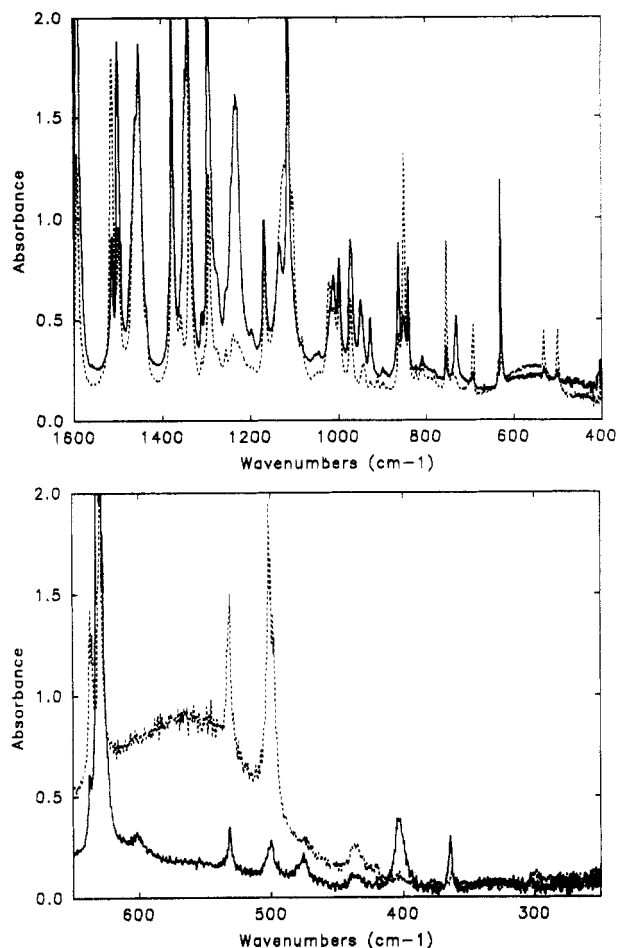


**Figure 4.** Polarized IR spectra of a PEO(D4)-pnp (100) spherulite: broken line, ⊥; solid line, ||.

**Table 4. Attributions, Dichroic Ratios, and  $\alpha$  Angles Observed for pnp IR Bands for Peripheral Part of a Spherulite of PEO(D4)-pnp Complex**

mode	wavenumber (cm <sup>-1</sup> )	dichroic ratio	$\alpha$ (deg)
a <sub>1</sub>			
20a	364	3.44	37
6a	630		
9a	1166		
19a	1500		
8a	1612	4.13	35
b <sub>1</sub>			
16b	501	0.13	76
10b	635	⊥	
4	694	0.17	74
11	755	0.19	73
17b	851	0.11	77
5	959		
b <sub>2</sub>			
19b	1448		
8b	1589	2.56	41
20b	3084	0.17	74
$\nu(\text{OH})$	3271	5.25	32
wag	437		
rock	531	0.27	70
sciss	863	6.0	30
$\nu_{\text{as}}$	1512	0.32	68

polarized FTIR spectra of a PEO(D4)-pnp spherulite are given in Figure 4. Table 4 gives the observed dichroic ratios of the pnp vibrations, which are in agreement with the dichroic ratios observed for the hydrogenated complex (Table 3). The crystal structure of these two complexes is evidently assumed to be the same.

A large amount of data on the dichroism behavior of the PEO IR-active vibrations may be obtained because three distinct types of fibers and a doubly oriented sample were

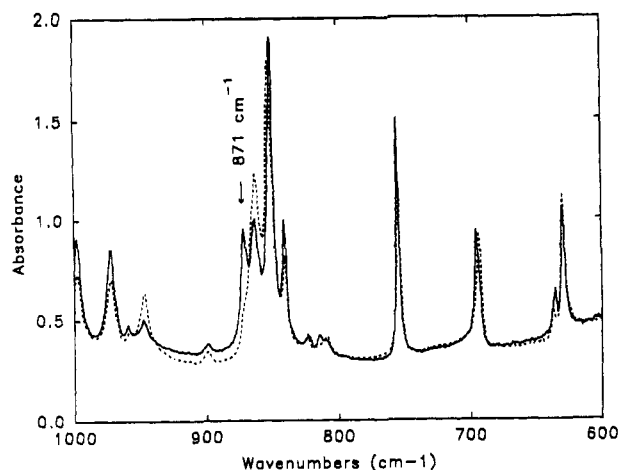


Figure 5. Polarized IR spectra of a PEO-pnp (010) spherulite: broken line,  $\perp$ ; solid line,  $\parallel$ .

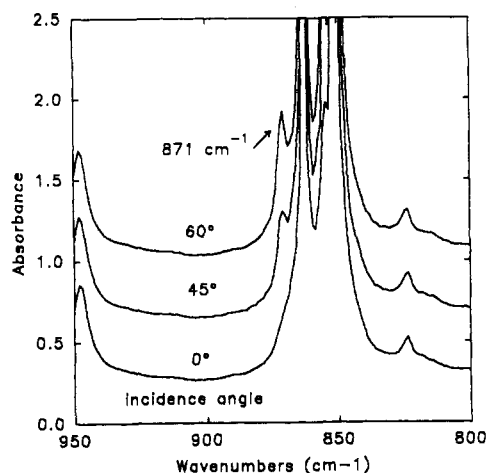


Figure 6. FTIR spectra of a doubly oriented sample of PEO-pnp complex measured at 0, 45, and 60° incidence angle.

prepared. First, by mechanical stretching of the samples, we obtained uniaxially oriented films with a  $c$  axis. Second, the spherulites grown at crystallization temperatures below 58 °C or above 65 °C show a (100) crystallographic growth face normal to the spherulite radius. The diffraction pattern of a peripheral part of such a spherulite corresponds to a fiber diagram with an  $a^*$  axis.<sup>21</sup> Third, the spherulites grown at crystallization temperatures between 58, and 65 °C show a (010) crystallographic growth face. The diffraction pattern of a peripheral part of these spherulites is a fiber diagram with a  $b^*$  axis.<sup>21</sup> Finally, doubly oriented specimens were prepared by stretching very thin and poorly crystalline films of the complex. The X-ray diffraction patterns obtained for three orientations of the incident beam have shown that the  $c$  and  $a^*$  crystallographic parameters of the crystals are in the plane of the samples.<sup>3</sup>

The polarized FTIR spectra obtained for stretched samples, (100) spherulite, and (010) spherulite are given in Figures 1, 3, and 5, respectively. Tables 5 and 6 give the IR wavenumbers and the dichroic behavior of the PEO and PEO(D4) IR bands, respectively. From an experimental point of view, the IR vibrations of the PEO chains may be classified in three groups according to the dichroism observed for the different samples. Considering hydrogenated samples, first, the 457-, 841-, 1032-, 1135-, 1310-, 1385-, and 1472- $\text{cm}^{-1}$  bands are polarized parallel in the (100) spherulites. Second, the 871- and 1036- $\text{cm}^{-1}$  vibrations are polarized parallel in the (010) spherulites. Third, the 950- and 1248- $\text{cm}^{-1}$  vibrations are polarized parallel

Table 5. Observed Wavenumbers and Dichroism of PEO Vibrations in the Complex

wavenumber <sup>a</sup> ( $\text{cm}^{-1}$ )	dichroism		
	stretched specimens	(100) spherulites	(010) spherulites
w 158	$\parallel$		
vw 207	$\perp$		
vw 237			
br 300			
m 457	$\perp$		$\perp$
m 871	$\perp$	$\perp$	$\parallel$
sh 841	$\perp$	$\parallel$	$\parallel$
m 950	$\parallel$	$\perp$	$\perp$
s 1032	$\perp$	$\parallel$	$\perp$
m 1036	$\perp$	$\perp$	$\parallel$
s 1135	$\perp$	$\parallel$	$\perp$
m 1248	$\parallel$		$\perp$
w 1310	$\perp$	$\parallel$	$\perp$
m 1385	$\perp$	$\parallel$	$\perp$
s 1472	$\perp$	$\parallel$	$\perp$

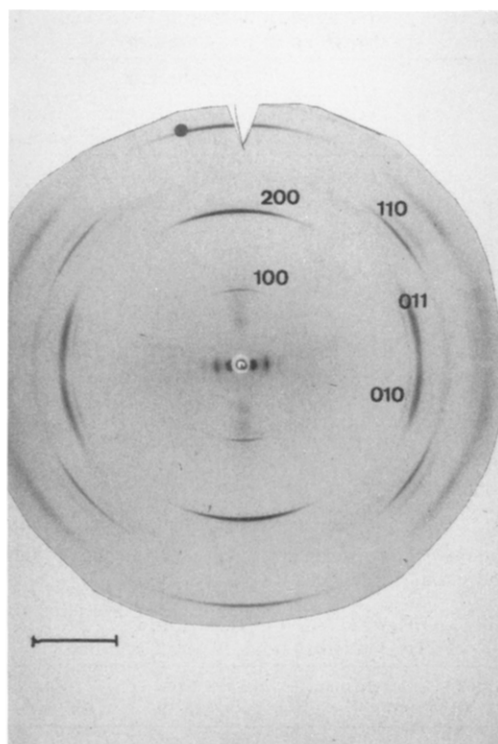
<sup>a</sup> vw = very weak, w = weak, m = medium, s = strong, sh = shoulder, br = broad band.

Table 6. Observed Wavenumbers and Dichroism of PEO(D4) Vibrations in the Complex

wavenumber ( $\text{cm}^{-1}$ )	dichroism (100) spherulites	wavenumber ( $\text{cm}^{-1}$ )	dichroism (100) spherulites
w 145		w 914	$\perp$
w 186		s 931	$\parallel$
w 245		s 947	$\perp$
m 404	$\parallel$	m 951	$\parallel$
w 476	$\parallel$	m 1015	$\parallel$
vw 600	$\parallel$	m 1024	$\perp$
vw 710		vw 1048	$\parallel$
sh 742	$\perp$	w 1082	$\perp$
s 733	$\parallel$	s 1134	$\parallel$
w 781	$\perp$	w 1253	

in stretched films, and, then, the transition moment is along the chain axis. Pleochroism measurement on doubly oriented films has confirmed the polarization of the 871- $\text{cm}^{-1}$  vibration. Figure 6 gives the IR spectra of such a film, the incidence angles between the normal to the film and the IR beam being 0, 45, and 60°. It appears very clearly from the increase of the 871- $\text{cm}^{-1}$  band intensity with the tilt angle that its direction of polarization is nearly perpendicular to the plane of the film ( $a^*$ ,  $c$  plane).

**Remark about the Orientation of the Chain Axis of the PEO Molecules.** All previously obtained evidence on our PEO-pnp complex leads to the assumption that the chain axis is actually along the  $c$  crystallographic parameter parallel to the stretching direction and perpendicular to the spherulite radius. In pure PEO and in many polymer crystals the vibrations polarized perpendicular to the chain axis are degenerated. Thus, in such crystals parallel dichroism in spherulites is unexpected, except if these vibrations appear as a doublet, resulting from intermolecular interactions (Davidoff splitting). For instance, in the PEO-*p*-dihalogenobenzene intercalates, the factor group of the PEO chains is isomorphous with the dihedral group  $D(6\pi/10)$  for which the  $E_1$  vibrations are doubly degenerated. However, due to the interactions in the crystal, these  $E_1$  vibrations appear experimentally as a doublet of two nondegenerated vibrations with distinct polarization directions.<sup>22</sup> In the (100) spherulites of the PEO-pnp complex, numerous vibrations which are not components of doublets are polarized parallel to the spherulite radius (with large dichroic ratios). Such an unusual feature would be easily explained if, in contradiction to our previous conclusions, the chain axis of the PEO molecules was assumed to be aligned with the



**Figure 7.** X-ray diffraction pattern (WAXS and SAXS) of a spherulite of  $\alpha$ -dodecyl- $\omega$ -hydroxytetracos(ethylene oxide)-pnp complex. Scale bar corresponds to  $1 \text{ nm}^{-1}$  with  $\lambda = 0.15418 \text{ nm}$ .

spherulite radius. The observation of negative spherulites does not rule out this assumption because PEO is the minor component of the complex (32% by weight). Therefore, we decided to confirm the orientation of the chains in the unit cell. The X-ray diffraction pattern of a spherulite of Brij 35 ( $\alpha$ -dodecyl- $\omega$ -hydroxytetracos(ethylene oxide))-pnp (Figure 7) has given this confirmation. The indexing of the WAXS pattern shows that in the Brij 35-pnp spherulites, the crystals exhibit the same structure and the same orientation as in ordinary PEO-pnp spherulites. The SAXS pattern of Figure 6, the intensity of which is enhanced by the presence of the paraffinic part of Brij 35 molecules, shows that, as usual, the normal to the limiting plane of the lamellae is normal to the spherulite radius.

**Factor Group of the PEO Macromolecules.** Vibrations of the PEO chains in the PEO-pnp complex are polarized along either the  $c$ ,  $a^*$ , or  $b$  crystallographic parameters. To explain that numerous vibrations are polarized along the  $a^*$  reciprocal parameter, we have assumed that either the (100) would be a symmetry glide plane or the  $a^*$  parameter would correspond to a symmetry axis. If  $D_2$  or  $C_s$  factor groups are assumed, too many vibrations would be expected ( $32B_1 + 32B_2 + 32B_3$  for  $D_2$  and  $63A' + 63A''$  for  $C_s$ ). But the fact that seven bands are polarized parallel to  $a^*$  and that only two bands are polarized along  $c$  and  $b$  leads us to assume the  $C_{2h}$  factor group, where  $a^*$  and the plane ( $b,c$ ) are the symmetry axis and the glide plane, respectively (Figure 8). Thus, the directions of polarization of  $871$  and  $947 \text{ cm}^{-1}$  may be everywhere in the ( $b,c$ ) plane. Nevertheless, the number of active vibrations ( $31A_u + 32B_u$ ) remains fairly large, but a part of the spectra characteristic of the PEO chains is overlapped by strong pnp IR bands.

The assumption of  $C_{2h}$  symmetry may also be confirmed by a discussion of the stoichiometry of the complex. With such a symmetry group, the six monomeric units contained in a repeat period are included in two components of three monomers having the same conformation related to one

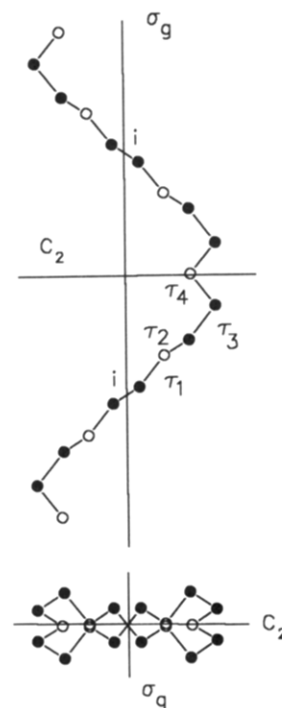


**Figure 8.** Symmetry of the  $(t_2gt_2gt_3t_2g't_2g't_3)$  conformation.

**Table 7. Proposed Conformations, Period, and Intramolecular Energy**

conformation $-C-\tau_1-O-\tau_2-C-\tau_3-C-\tau_4-O-$	repeat period (nm)	intramolecular energy (kcal/mol of monomeric unit)
tggt	1.53	2.5
tggt	1.75	2.8
ttgg	1.75	2.5
ttgt	1.61	-2.3
tttg	1.53	2.7

another by the glide plane and the  $C_2$  axis. To each of these components would be associated a pair of pnp molecules. In fact, we have assumed that the pnp molecules, which are not symmetrically disubstituted in para positions, form pairs of molecules.

**Conformation of the PEO Macromolecules.** On the basis of the  $C_{2h}$  factor group, only four torsion angles are needed to completely determine the chain conformation (Figure 8). Table 7 summarizes the conformations which give a low value of the intramolecular energy and which may be in accordance with the crystallographic data ( $1.557 \text{ nm}/6$  monomeric units) by small adjustments of the torsion angles. We have assumed torsion angles strictly equal to  $60^\circ$ ,  $180^\circ$ , and  $300^\circ$  (g, t, and g', respectively). From Table 7, the  $(t_2gt_2gt_3t_2g't_2g't_3)$  glide conformation given in Figure 8 has the smallest intramolecular energy. Note also that the (ttg) and (ttt) conformers are well known to be especially stable in the case of PEO.<sup>23,24</sup> We have then calculated the normal modes of vibration for these different molecular models, and here again the best agreement between observed and calculated frequency (Table 8) is obtained for the energetically stable  $(t_2gt_2gt_3t_2g't_2g't_3)$  conformation. As previously indicated, the directions of the dipole moment observed for the  $947\text{-cm}^{-1}$  vibration, polarized along the  $c$  parameter, and the  $871\text{-cm}^{-1}$  vibration, polarized along  $b$ , do not result from the symmetry of the molecule. To confirm our proposal, J. Libert (Service des Matériaux Nouveaux, Professor Brédas of our University) has calculated the orientation of the transition dipole moment for both these vibrations by an ab initio

**Table 8. Observed and Calculated Wavenumbers for Hydrogenated and Deuterated PEO Chains in the (t<sub>2</sub>gt<sub>2</sub>gt<sub>2</sub>t<sub>2</sub>g't<sub>2</sub>g't<sub>2</sub>) Conformation**

PEO		PEO(D4)	
obsd wavenumbers (cm <sup>-1</sup> )	calcd wavenumbers (cm <sup>-1</sup> )	obsd wavenumbers (cm <sup>-1</sup> )	calcd wavenumbers (cm <sup>-1</sup> )
A <sub>u</sub> Modes of Vibrations			
	185	117	118
237	245		166
300	328		204
457	436	300	302
	576	404	387
	824	476	514
841	843	600	613
	896	710	690
1032	1042	733	752
	1083		867
	1115		875
1135	1137		898
	1219	931	940
	1239	951	949
	1267	1015	993
1310	1291	1048	1038
	1338		1067
1385	1389		1087
	1445		1121
	1454	1134	1133
1472	1473	1253	1260
B <sub>u</sub> Modes of Vibrations			
158	154	145	138
	196	186	177
300	315	245	277
	486		429
	542		478
	834		614
	874	742	734
950	948	781	771
1036	1044		877
1088	1099	914	905
	1107		937
	1150	947	946
	1223	947	949
1248	1253		992
	1273	1024	1005
1310	1291		1061
	1339	1082	1066
	1399		1103
	1444		1105
	1451		1129
1472	1464	1253	1243

method. The calculated direction cosines of the vibrations are  $M_x = 0.0$ ,  $M_y = 0.9996$ , and  $M_z = -0.0284$  for  $871\text{ cm}^{-1}$  and,  $M_x = 0.0$ ,  $M_y = 0.3187$ , and  $M_z = -0.9478$  for  $950\text{ cm}^{-1}$ . The  $x$  and  $z$  axes correspond to the  $C_2$  symmetry axis and the chain axis, respectively. These calculations are in agreement with the observed dichroism of the PEO molecules. In fact, the  $871\text{-cm}^{-1}$  band is very strongly polarized (Figure 5), and then its transition moment is actually along  $b$ . On the contrary, the  $950\text{-cm}^{-1}$  band is polarized with a low dichroic ratio (equal to 3, Figure 1), and then its transition moment makes an angle lower than  $39^\circ$  with the  $c$  parameter. Thus, several experimental facts and theoretical considerations give us confidence that  $(t_2\text{-}gt_2gt_3t_2g't_2g't_3)$  is the glide conformation for the PEO chains in the complex. The final crystal structure proposed on the basis of spectroscopic arguments is given in Figure 9.

## Conclusions

By using polarized IR spectroscopy, we can propose a model for the crystalline structure of the PEO-pnp complex. From the FTIR spectra of stretched and spherulitic samples, we have determined the orientation

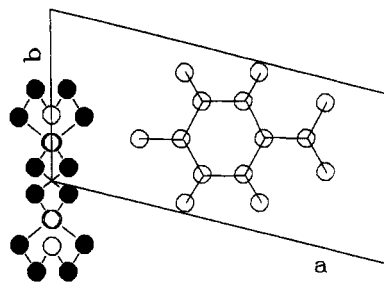


**Figure 9.** Crystal structure proposed for the PEO–pnp molecular complex.

of the pnp molecules in the unit cell and the conformation of the PEO chains. The benzene rings are found to be perpendicular to the *c* crystallographic parameter (chain axis) and the 1–4 axis of the pnp molecules is parallel to the *a*\* reciprocal parameter. The (*t*<sub>2</sub>*g**t*<sub>2</sub>*g**t*<sub>2</sub>*g**t*<sub>2</sub>*g*) conformation is derived from the crystallographic data, from energy and symmetry considerations, and from normal mode analyses. However, we do not know, at the present time, if the crystalline structure is centrosymmetric or not (as concerns the pnp molecules).

**Acknowledgment.** This work was supported by the Ministère de la Région Wallonne, Programme de Formation et d'Impulsion à la Recherche Scientifique et Technologique, and by the F.N.R.S. (Fonds National de la Recherche Scientifique, Belgium). We acknowledge J. Libert (Service des Matériaux Nouveaux, Professor Brédas, University of Mons) for his assistance in the ab initio calculations of the transition moments.

## References and Notes

- (1) Iwamoto, R.; Saito, Y.; Ishihara, H.; Tadokoro, H. *J. Polym. Sci., Part A-2* **1968**, *6*, 1509.
- (2) Point, J. J.; Coutelier, C. *J. Polym. Sci., Polym. Phys. Ed.* **1985**, *23*, 231.
- (3) Point, J. J.; Damman, P. *Macromolecules* **1992**, *25*, 1184.
- (4) Cooper, D. R.; Leung, Y. K.; Heatley, F.; Booth, C. *Polymer* **1978**, *19*, 309.
- (5) Zbinden, R. *IR Spectroscopy of High Polymers*; Academic Press: New York, 1964.
- (6) Fraser, R. D. B. *J. Chem. Phys.* **1958**, *28*, 1113.
- (7) Beer, M. *Proc. R. Soc. London* **1956**, *A236*, 136.
- (8) Point, J. J.; Jasse, B.; Dosière, M. *J. Phys. Chem.* **1986**, *90*, 3273.
- (9) Randle, R. R.; Whiffen, D. H. *J. Chem. Soc.* **1952**, 4153.
- (10) Stephenson, C. V.; Coburn, W. C.; Wilcox, W. S. *Spectrochim. Acta* **1961**, *17*, 933.
- (11) Green, J. H. S.; Harrison, D. J.; Kynaston, W. *Spectrochim. Acta* **1971**, *27A*, 2199.
- (12) Pinchas, S.; Samuel, D.; Silver, B. L. *Spectrochim. Acta* **1964**, *20*, 179.
- (13) Garrigou-Lagrange, C.; Lebas, J. M.; Josien, M. L. *Spectrochim. Acta* **1958**, *12*, 305.
- (14) Green, J. H. S.; Kynaston, W.; Lindsey, A. S. *Spectrochim. Acta* **1961**, *17*, 486.
- (15) Evans, J. C. *Spectrochim. Acta* **1960**, *16*, 1382.
- (16) Wilson, E. B.; Decius, J. C.; Cross, P. C. *Molecular Vibrations*; McGraw Hill: New York, 1955.
- (17) Shimanouchi, T.; Harada, I. *J. Chem. Phys.* **1964**, *41*, 2651.
- (18) Tadokoro, H.; Chatani, Y.; Yoshihara, T.; Tahara, S.; Murahashi, S. *Makromol. Chem.* **1964**, *73*, 109.
- (19) Pimentel, G. C.; Sederholm, C. H. *J. Chem. Phys.* **1956**, *24*, 639.
- (20) Coppens, P.; Schmidt, G. H. *J. Acta Crystallogr.* **1965**, *18*, 654.
- (21) Damman, P.; Point, J. J. *Macromolecules* **1993**, *26*, 1722.
- (22) Point, J. J.; Damman, P. *Macromolecules* **1991**, *24*, 2019.
- (23) Flory, P. J. *Statistical Mechanics of Chain Molecules*; Interscience: New York, 1969.
- (24) Smith, G. D.; Yoon, D. Y.; Jaffe, R. L. *Macromolecules* **1994**, *26*, 5213.